Noise-Sustained Pulsating Patterns and Global Oscillations in Subexcitable Media

H. Hempel,[1] L. Schimansky-Geier,[1] and J. García-Ojalvo[1,2]

[1]*Institut für Physik, Humboldt-Universität zu Berlin, Invalidenstrasse 110, D-10115 Berlin, Germany*
[2]*Departament de Física i Enginyeria Nuclear, Universitat Politècnica de Catalunya, Colom 11, E-08222 Terrassa, Spain*
(Received 30 November 1998)

The constructive role of noise in an excitable activator-inhibitor medium is analyzed. Noise acts parametrically on the excitation threshold of the system, and is seen to support the existence of pulsating spots in the subexcitable regime. Increasing values of the noise intensity in this regime lead to a collective state in which all the elements of the system fire synchronously. The spectral characteristics of the resulting global oscillations are also studied as a function of the noise intensity, showing the typical fingerprint of stochastic resonance. [S0031-9007(99)09016-X]

The ordering role of noise in the dynamics of nonequilibrium systems is a well-established fact. Both temporal [1] and spatiotemporal [2] systems have been seen to become influenced in a constructive way by the action of external fluctuations. Phenomena such as stochastic resonance [3] and noise-induced transport [4] are well-known examples of the beneficial effects of fluctuations in nonlinear dynamical systems. Additionally, spatial coupling has been found to enhance the ordering properties of external noise. Examples of this fact are noise-induced nonequilibrium phase transitions [5] and array-enhanced stochastic resonance [6].

From a deterministic point of view, the spatiotemporal behavior of excitable media has attracted much attention in recent years. These systems exhibit a very rich phenomenology, including traveling pulses, spiral waves, and twisted scrolls [7]. Such structures have been observed in a large variety of biological, chemical, and physiological systems [8]. The recent observations of noise-supported traveling waves in the photosensitive Belousov-Zhabotinsky reaction [9] and of noise-induced spiral waves in cultured networks of rat brain cells [10] have directed the attention towards the relevance of noise in these systems.

The question that we aim to address in this Letter is twofold. First, we intend to delve into the study of the ordering role of spatiotemporal noise in the important class of excitable media. These systems are specially sensitive to external noise [9], but a theoretical understanding of the mechanisms by which this order arises is still lacking and requires more experimental and numerical investigations. The phenomena described in what follows could help to shed some light into the origin of these mechanisms. Second, the constructive influence of noise might lead to the existence of excitation patterns in neural systems such as cortical tissue. There, background fluctuations are much more important than in physical or chemical systems [11]. Patterns and synchronous behavior of excitation in neural systems have been observed experimentally [10,12] and predicted in several models [13,14]. However, only a few

investigations [10,15] have pointed out that background noise in an excitable medium could be responsible for those patterns.

In order to face the questions posed above, we analyze in this paper a model of excitable media with activator-inhibitor dynamics. Activator-inhibitor models have been recently used to examine the influence of noise in excitable systems. The spatially homogeneous FitzHugh-Nagumo model has been seen, for instance, to exhibit noise-enhanced coherent response both in autonomous situations [16] and in the presence of an additional external periodic signal [17]. In the following we use instead a *cellular automaton* model, with the aim of examining the influence of parametric noise in subexcitable media. Cellular automata (CA) have been frequently used to represent the dynamics of excitable media [18] and provide a realistic description of cortical tissue [13]. A CA-based implementation of an array of stochastic threshold devices with excitable properties was proposed by Jung and Mayer-Kress (JM) [15]. Their results showed that noise was able to sustain spiral growth, leading to the first evidence of spatiotemporal stochastic resonance in excitable media [19]. The JM model introduces an *ad hoc* refractory period and does not account for inhibitor dynamics. Therefore, it cannot describe the rich variety of structures (e.g., spots, Turing patterns) that appears when the inhibitor diffuses faster than the activator [7]. Here we present a CA model that explicitly describes the dynamics of the two species (activator and inhibitor), allowing both of them to diffuse. As we will show in what follows, parametric noise supports in this model the existence of pulsating patterns [13] and synchronized global oscillations in the subexcitable regime. We should remark that this second scenario, while being a remarkable example of collective behavior induced by noise, could be detrimental to the operation of a neural system, which usually relies on localized excitations [11]. It is therefore important to establish the conditions under which it occurs.

Our model is described by two dynamic variables, u_{ik} and v_{ik}, defined in a two-dimensional square lattice with

$N \times N$ sites ($i, k = 1, \ldots, N$). The variable u_{ik}, which can take only the values 0 or 1, represents the state of the activator at a given cell: When it is equal to 1 the cell is in an excited state, and when it is equal to 0 it is in a resting state. The second variable, v_{ik}, represents the inhibitor concentration, as measured by a number of particles that act on the state u_{ik} inhibitorically.

The activator obeys the following threshold dynamics:

$$u_{ik}(t + \Delta t = H[\langle u(t)\rangle_{ik} - a_{ik}], \qquad (1)$$

where H is the Heaviside step function that is equal to 1 whenever $\langle u(t)\rangle_{ik} > a_{ik}$ and 0, otherwise. Hence the parameter a_{ik} represents the local excitation threshold of the system, which is assumed to increase with inhibitor concentration and to be subject to spatiotemporal fluctuations, according to $a_{ik} = a_0 + \beta v_{ik}(t) + \sigma \xi_{ik}(t)$, where a_0 is a constant contribution to the threshold level, β represents coupling to the inhibitor, and σ is the standard deviation of the noise, which obeys a Gaussian distribution and is uncorrelated both in space and time. Note that a cell fires depending not on its local state, but on the value of a local spatial average represented by the bracket notation $\langle \cdots \rangle_{ik}$. This average is defined by $\langle u(t)\rangle_{ik} = \sum_{i'k'} u_{i'k'}(t) K(i', k', i, k)$, where the sum in the previous expression runs over all sites in the lattice, and $K(i', k', i, k)$ is a normalized kernel that depends only on the Euclidean distance between sites (i, k) and (i', k'). We have chosen an approximately Gaussian kernel (see Fig. 1 of Ref. [18]). The previous average corresponds to a local density of active sites in the neighborhood of a given cell (i, k). According to rule (1), this cell becomes excited if the corresponding local density is overcritical at the previous time instant. A spatial coupling is thus realized due to this rule. The characteristic length L_u of this coupling (corresponding to the diffusion length of the activator) is controlled by the width of the Gaussian kernel $K(i', k', i, k)$. The relaxation time τ_u of the activator in this model will be given, according to the dynamical rule (1), by the integration time step, $\tau_u = \Delta t$.

The definition of the threshold parameter a_{ik} given above establishes the inhibitory character of v_{ik}: the larger its value, the higher the excitation threshold. As stated above, this variable corresponds to the number of inhibitory particles, and its dynamics is described by a set of birth-death rules that update the value of v_{ik} every time step Δt. Birth processes are governed by a deterministic rule: In all excited sites the number of particles increases by a constant amount $\gamma b^2 \Delta t$, where γ is a generation rate per unit area, and b is the lattice spacing. Death processes follow a probabilistic precept: At every update, a particle decays with constant probability $\Delta t/\tau_v$, where τ_v is the decay time of v. Additionally, the particles exhibit a random walk on the lattice, realized by several jumping processes every time step which in the end approximate a Gaussian distribution of jumps. The characteristic length L_v of this random walk is a measure of the diffusion length of the inhibitor.

We stress again at this point that the new feature of the present model with respect to that of JM is the dynamics of the inhibitor, which implies that the refractory time is no longer a constant parameter of the model, but is determined by the dynamics of the system itself. Furthermore, the inhibitor is able to diffuse through the lattice, introducing a second mechanism of intercell coupling that gives rise to a much richer variety of structures [7]. In particular, the presently proposed algorithm is able to reproduce, in the absence of external noise ($\sigma = 0$), all known typical patterns appearing in excitable media, such as spiral waves, spots, stationary periodic and labyrinthic patterns, etc. [20]. The regime in which the system evolves is basically determined by the parameters $\epsilon \equiv \tau_u/\tau_v$ and $\alpha \equiv D_u/D_v$, where $D = L^2/\tau$ is the diffusion coefficient of the corresponding species. In particular, two well-established limits [7] can be observed: For small ϵ and large α the system develops spiral waves; in the opposite case of large ϵ and small α standing patterns of spots are observed. In the intermediate region, nonstationary (turbulent) patterns can be found.

We are interested in examining the influence of noise in the subexcitable regime, in which no initial structure can survive deterministically. Common parameters that will be used throughout all our investigation are $N = 128$, $\Delta t = 1$, $a_0 = 0.14$, $\gamma \tau_v = 190$, and $\beta = 4.2 \times 10^{-3}$. The choices $\epsilon = 0.25$ and $\alpha = 0.5$ correspond to a subexcitable situation. Periodic boundary conditions are considered. The typical evolution of a localized initial condition is shown in Fig. 1 for increasing values of the noise level σ. Different rows correspond to different values of σ; within each row time evolves towards the right.

For small noise intensities (top row), the initial perturbation begins to spread and a ring pattern develops, but the structure finally decays as the system reaches a steady rest state where all cells are inactive. A *survival time* can be defined as the time during which the structure exists. As soon as a small amount of fluctuations is added to the threshold parameter, a constructive influence of noise can be observed in the form of an increase in the survival time of the structures. This occurs through the breakup of the initial ring into several spots, one or several of which can grow and give rise to further rings that may break up into other spots, and so on.

The survival time (and the number of spots that experience growth and breakup) increases with the noise level σ. Beyond a certain critical value of this parameter ($\sigma_1 \approx 4.5 \times 10^{-2}$), the structures were not observed to decay in our longer simulation times (10 000 time steps). This situation is shown in the second row from the top in Fig. 1. If fluctuations are switched off, the spots disappear within the survival time corresponding to $\sigma = 0$. Therefore, these pulsating structures (also observed in a physiological context [13]) are *sustained* by noise. Three
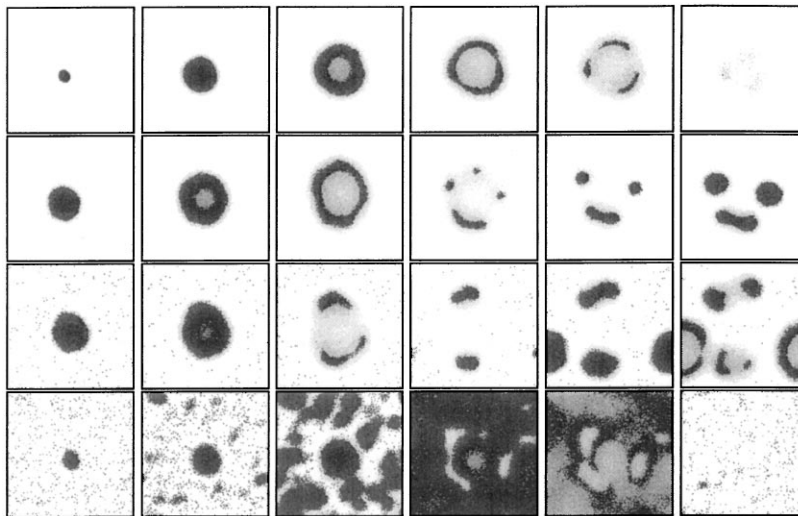
FIG. 1.   Time sequences for different scenarios (time flows from left to right).   From top: first sequence—subcritical noise ($\sigma = 1.6 \times 10^{-2}$); second sequence—noise-sustained structures ($\sigma = 4.7 \times 10^{-2}$); third sequence—spontaneous nucleation and global oscillations ($\sigma = 5.7 \times 10^{-2}$); fourth sequence—synchronized oscillations ($\sigma = 6.3 \times 10^{-2}$).   Black denotes excitation ($u_{ik} = 1$) and the gray level corresponds to inhibitor concentration (the darker the cell, the higher the concentration).   Note that the time interval between consecutive snapshots differs in general.

remarks should be made concerning these noise-sustained spots.   First, an inhomogeneous initial condition is required for these structures, since noise is not large enough to induce spontaneous nucleation that seeds the spots. Second, the spots require a minimal system size to develop; they do not survive for small system sizes.   Third, the noise-sustained structures exist provided noise acts independently in the different sites of the lattice (spatially uncorrelated noise).   A *global* noise, affecting in an identical way all lattice cells every time instant, is not able to sustain structures in this system (spatial correlation is well known to reduce the constructive effect of noise; see, for instance, [2]).

Beyond a second threshold $\sigma_2 \approx 5.5 \times 10^{-2}$, spontaneous nucleation occurs (third row from the top in Fig. 1). In this regime no particular initial condition is required for the structures to appear, since noise is large enough to generate perturbations that seed the spots.   Furthermore, one can observe in this scenario the existence of oscillations of the global signal $U(t) = \sum_{ik} u_{ik}(t)/N^2$.   The power spectrum of this global signal is shown in the left plot of Fig. 2.   The oscillations are seen to possess a well-defined main frequency; both this frequency and the oscillation amplitude increase with the noise level σ.   The local signal $u_{ik}(t)$, on the other hand, does not show a regular oscillatory behavior (its power spectrum does not reveal any particular dominant frequency; see right plot of Fig. 2).

Finally, for noise levels larger than $\sigma_3 \approx 6.0 \times 10^{-2}$ (lower row of Fig. 1), nucleation processes become more frequent, leading to a high degree of synchronization between firing events in the different sites of the lattice. Therefore, even though the deterministic system is located

in a subexcitable regime, noise induces the medium to become oscillatory.   In the case shown in the bottom row of Fig. 1, synchronization is not complete, and several nucleation processes all through the lattice can be distinguished in the prefiring step (third snapshot).   Synchronization improves for increasing noise until finally, when the nucleation time becomes much smaller than the intrinsic refractory time of the system, all cells fire and come back to rest basically at the same time (see Fig. 3).   In this regime, also the local signal oscillates with a well-defined frequency.

The dependence of the oscillatory properties of the system on the noise amplitude σ is shown in Fig. 4, in terms of the height and position of the global-signal spectral peak shown in the left plot of Fig. 2.   The former quantity measures the amplitude of the oscillations, which exhibits a maximum for a certain optimal noise, corresponding to perfect synchronization of the firing events. For larger noise levels, synchronization is destroyed by
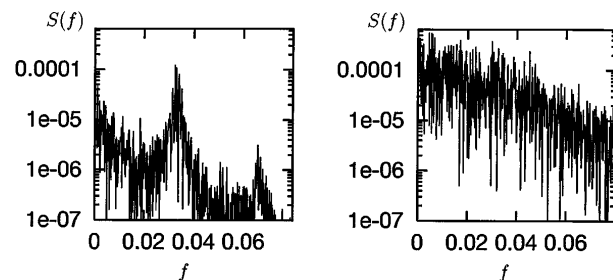

FIG. 2.   Power spectra $S(f)$ of the global (left) and local (right) signals at the onset of the oscillatory regime ($\sigma = 5.7 \times 10^{-2}$—third row from the top in Fig. 1).
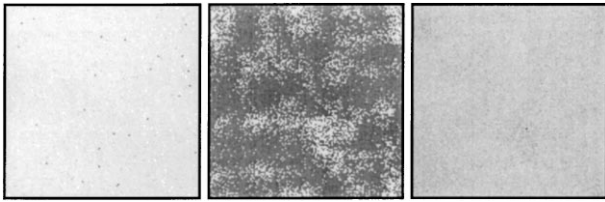
FIG. 3. Time sequence for a large noise level ($\sigma = 0.12$). As in Fig. 1, time flows from left to right, and the sequence repeats again after the third snapshot.

fluctuations. On the other hand, the frequency of the oscillations (as measured by the position of the spectral peak—right plot of Fig. 4) is seen to increase monotonously with noise strength, reaching a saturation level that decreases with the inhibitor's decay time τ_v (compare diamonds and crosses in the right plot of Fig. 4).

Figure 4 also displays the results corresponding to the power spectrum of the local signal $u_{ik}(t)$ (squares), which basically coincide with those of the global output discussed above. This means that basically in the whole range of noise strengths presented in this figure (precisely for $\sigma > \sigma_3 = 6.0 \times 10^{-2}$, i.e., all points in the figure except the leftmost ones), synchronization ensures that both the local and the global fields oscillate with the same well-defined frequency. We should also note that the previous results do not depend on the ability of the inhibitor to diffuse: they hold even in the limiting case $L_v = 0$. However, the scenarios shown in Figs. 1 and 3 are not observed in models with fixed refractory time, such as the JM model. This fact leads to the conclusion that it is the local dynamics of the inhibitor and the associated *dynamical* refractory time of the system that gives rise to the noise-sustained spots, global oscillations, and noise-induced synchronization phenomena that have been

described above. However, a quantitative explanation of these phenomena is still needed.
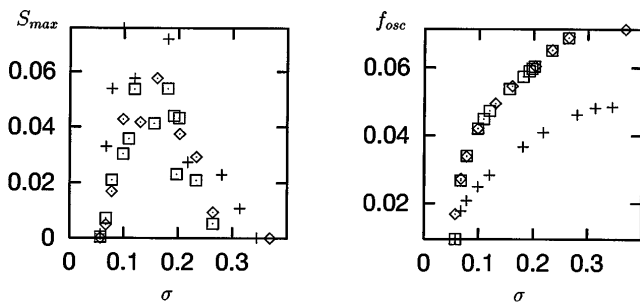
FIG. 4. Amplitude (left) and frequency (right) of the oscillating global (diamonds and crosses) and local (squares) signal as a function of the noise level σ. Diamonds and squares: $\epsilon = 0.25$; crosses: $\epsilon = 0.12$.

[1] W. Horsthemke and R. Lefever, *Noise-Induced Transitions* (Springer-Verlag, Berlin, 1984).
[2] J. García-Ojalvo and J. M. Sancho, "Noise in Spatially Extended Systems" (Springer, New York, to be published).
[3] L. Gammaitoni, P. Hänggi, P. Jung, and F. Marchesoni, Rev. Mod. Phys. **70**, 223 (1998).
[4] P. Hänggi and R. Bartussek, in *Nonlinear Physics of Complex Systems,* edited by J. Parisi, S. C. Müller, and W. Zimmermann (Springer-Verlag, Berlin, 1996).
[5] C. Van den Broeck, J. M. R. Parrondo, and R. Toral, Phys. Rev. Lett. **73**, 3395 (1994); J. García-Ojalvo, J. M. R. Parrondo, J. M. Sancho, and C. Van den Broeck, Phys. Rev. E **54**, 6918 (1996).
[6] J. F. Lindner, B. K. Meadows, W. L. Ditto, M. E. Inchiosa, and A. R. Bulsara, Phys. Rev. Lett. **75**, 3 (1995); M. Löcher, G. A. Johnson, and E. Hunt, Phys. Rev. Lett. **77**, 4698 (1996); U. Siewert and L. Schimansky-Geier, Phys. Rev. E **58**, 2843 (1998).
[7] A. Mikhailov, *Foundations of Synergetics* (Springer-Verlag, Berlin, 1994).
[8] A. T. Winfree, *When Time Breaks Down* (Princeton University Press, Princeton, NJ, 1987).
[9] S. Kádár, J. Wang, and K. Showalter, Nature (London) **391**, 770 (1998); J. Wang, S. Kádár, P. Jung, and K. Showalter, Phys. Rev. Lett. **82**, 855 (1999).
[10] P. Jung, A. Cornell-Bell, K. Madden, and F. Moss, J. Neurophysiol. **79**, 1098 (1998).
[11] D. J. Amit and N. Brunel, Cereb. Cortex **7**, 237 (1996).
[12] R. Llinas and U. Ribary, Proc. Natl. Acad. Sci. U.S.A. **90**, 2708 (1993); M. A. Whittington, R. D. Traub, and J. G. R. Jefferys, Nature (London) **373**, 612 (1995).
[13] W. M. Kistler, R. Seitz, and J. Leo van Hemmen, Physica (Amsterdam) **114D**, 273 (1998).
[14] C. C. Chow, Physica (Amsterdam) **118D**, 343 (1998).
[15] P. Jung and G. Mayer-Kress, Chaos **5**, 458 (1995).
[16] A. S. Pikovsky and J. Kurths, Phys. Rev. Lett. **78**, 775 (1997).
[17] A. Longtin and D. R. Chialvo, Phys. Rev. Lett. **81**, 4012 (1998); A. Neiman, L. Schimansky-Geier, F. Moss, B. Shulgin, and J. J. Collins (to be published).
[18] J. R. Weimar, J. J. Tyson, and L. T. Watson, Physica (Amsterdam) **55D**, 309 (1992).
[19] P. Jung and G. Mayer-Kress, Phys. Rev. Lett. **74**, 2134 (1995).
[20] H. Hempel, T. Fricke, and L. Schimansky-Geier, in *Nonlinear Physics of Complex Systems* (Ref. [4]).